Contents lists available at UGC-CARE

International Journal of Pharmaceutical Sciences and Drug Research

[ISSN: 0975-248X; CODEN (USA): IJPSPP]

journal home page : http://ijpsdr.com/index.php/ijpsdr

Research Article

Formulation and Development of Voriconazole Tablets Containing Solid Dispersion with Enhanced Solubility, Dissolution and Bioavailability

Atish B Velhal*, Vijay R Salunkhe

KES's, Rajarambapu College of Pharmacy, Kasegaon, Sangli, Maharashtra, India

ARTICLE INFO

Article history:

Received: 19 January, 2024

Revised: 26 February, 2024

Accepted: 03 March, 2024

Published: 30 March, 2024

Keywords:

Voriconazole, Tamarind gum, Solid dispersion, Carboxymethylated tamarind gum, Bioavailability, Solubility.

DOI:

10.25004/IJPSDR.2024.160212

ABSTRACT

This research work enhances the solubility, dissolution and bioavailability of voriconazole which belongs to the BCS II class. Carboxymethyl tamarind gum was synthesized by using carboxymethylation of tamarind gum. The solid dispersion of voriconazole was developed using a kneading method followed by immediate-release tablets. Solid dispersion is characterized for solubility and instrumental analysis. Tablets were evaluated for dissolution study. Solid dispersions were confirmed by presence of distinctive peaks at 1745.58 cm^{-1} (C=O) and 1402 cm^{-1} (-COO-), using Infrared spectroscopy. A weight loss of 3.91 and 54.42% at 100°C and in the rage of 235 to 425°C was observed. ^{13}C-nuclear magnetic resonance spectrum of carboxymethyl tamarind gum displayed three distinct C1, -OH, and CH2O- group peaks. X-ray diffraction analysis confirmed that carboxymethyl tamarind gum exhibits an amorphous structure. Soild dispersion of voriconazole were developed using the kneading method, incorporating carboxymethyl tamarind gum. Compared to traditional methods, Solid dispersion formulated with carboxymethyl tamarind gum demonstrated a significant increase in solubility enhancement, ranging from 68.12 to 74.37-fold. Notably, the SD5 formulation exhibited complete release from the solid dispersion within 120 minutes. In rat models, voriconazole levels in the bloodstream were markedly elevated with the administration of solid dispersion. Furthermore, dissolution profiles of all formulation batches showed considerable improvement. These findings shed light on effective strategies for enhancing the dissolution and bioavailability of poorly soluble drugs, thus contributing to the advancement of drug delivery systems.

INTRODUCTION

Voriconazole (VRZ) is a modern azole antifungal medication used to effectively treat a range of fungal infections, including invasive aspergillosis, esophageal candidiasis, and severe fungal infections.[1] However, voriconazole faces challenges due to its properties as a lipophilic drug with low aqueous solubility (maximum 2.7 mg/mL). Consequently, it falls under the biopharmaceutics classification system (BCS) II. The limited solubility of VRZ in water contributes to its low bioavailability, which ultimately hampers its effectiveness in treating infections.[2] The development of suitable pharmaceutical formulations is crucial to address this significant issue. Solid dispersions (SD) are formulations where poorly soluble drugs, like VRZ, could be dispersed or dissolved in a hydrophilic polymer matrix. SD achieve this by increasing the drug's surface area available for dissolution, disrupting its crystalline structure, improving wettability and spreadability in release media, and forming the complex between drug and polymer thereby enhancing the mobility of the drug. These mechanisms facilitate faster dissolution and improved solubility of the drug.[3] Overall, SD offers an effective strategy to overcome the challenges of low solubility and limited bioavailability of BCS class II drugs, enhancing their therapeutic effectiveness.

Natural polymers from plants and animals offer advantages over synthetic polymers. They are biodegradable, renewable,

***Corresponding Author:** Mr. Atish B Velhal

Address: KES's, Rajarambapu College of Pharmacy, Kasegaon, Sangli, Maharashtra, India

Email ✉**:** atishvelhal@gmail.com

Tel.: +91-9881646969

Relevant conflicts of interest/financial disclosures: The authors declare that the research was conducted in the absence of any commercial or financial relationships that could be construed as a potential conflict of interest.

and sustainable, reducing environmental impact.[4] Natural polymers exhibit excellent biocompatibility and lower toxicity.[5] Tamarind gum polysaccharide (TGP) has a molecular weight of 1735 kDa, TGP is water-soluble and possesses unique characteristics. TGP's properties make it a valuable ingredient in various applications, particularly in pharmaceuticals and food industries, where its solubility and functional attributes are highly beneficial.[6] It is characterized by its biodegradability, biocompatibility, noncarcinogenicity, and non-irritating properties. These attributes make TGP a favorable choice for pharmaceutical pharmaceuticals and cosmetics. Due to its promising applications, TGP, a biopolymer, has garnered significant attention in the pharmaceutical, cosmetic, and food sectors. It has been extensively studied and utilized as an additive in different drug delivery systems, such as those designed for oral, intestinal, ophthalmic, buccal, and nasal administration.[7, 8]

Despite its widespread use in drug delivery formulations, tamarind gum (TG) does possess certain drawbacks. These include an unpleasant odor, lackluster color, limited water solubility, and rapid degradation when exposed to aqueous environments.[9] TG has undergone chemical modification with carboxymethyl, acetyl, hydroxyl alkyl, thiol, and functional groups to address these constraints. This derivatization process has led to the development of functionally modified tamarind gums that showed potential as pharmaceutical additives in advanced drug delivery systems. These modified tamarind gums offer improved stability, reduced degradability, and enhanced mechanical properties.[10] The carboxymethylated tamarind gum (CMTG) has wider benefits than TG. CMTG enhances water solubility, dissolution, and stability. These applications have the potential to improve therapeutic efficacy, optimize drug delivery profiles, and enhance patient outcomes.[11] However, the use of CMTG in solid dispersion is limited and very little research has been done in this area.

The use of CMTG in SD to increase solubility and bioavailability has been extensively studied. Creating a hydrophilic matrix improves absorption and dissolution.[12] Overall, CMTG in solid dispersions offers a versatile approach to address solubility challenges and improve drug delivery. We have undertaken this work to utilise it in the formulation of solid dispersions with enhanced solubility as well as dissolution rate through fast-dissolving tablets.

This research work offers significant pharmaceutical advantages by addressing the challenges associated with enhancing the solubility, dissolution, and bioavailability of VRZ, a drug belonging to BCS II class. Through the synthesis of CMTG and the development of SD using the kneading method, this study demonstrates remarkable improvements in solubility enhancement, dissolution rates, and bioavailability compared to traditional methods. Incorporating CMTG in SD formulations leads to a substantial increase in solubility enhancement, resulting in enhanced drug release and elevated circulating VRZ levels in the bloodstream. These findings underscore effective strategies for optimizing drug delivery systems, thereby advancing pharmaceutical research and development.

Materials And Methods

Materials

VRZ was gifted from a specific source. Tamarind kernel powder/gum (TG) was gifted by Chhaya Industries and is located in Barshi, Maharashtra. Partially hydrolysed polyvinyl alcohol was obtained from HiMedia Laboratories Pvt. Ltd. Dichloromethane (DCM) purchased from Merck Specialities Pvt. Ltd. Mumbai. Acetone and methanol procured from Avantor Performance Materials India Limited, Thane.

Methods

Carboxymethylation of tamarind gum

Dispersion of TG (0.050 mol) was prepared in a mixture of alkaline aqueous methanol (100 mL) containing 0.090 to 0.180 mol of NaOH. To this dispersion, solid monochloric acid (0.079–0.101 mol) was added under continuous stirring for 15 minutes. This conical flask was containing reaction mixture was positioned in a thermostatic water bath at 40 to 85°C. The process was permitted to continue for the intended length of time, which varied between 30 and 90 minutes. Throughout the reaction, the flask contents were intermittently shaken. Once the reaction was complete, the resulting product was separated by filtration using a G-3 sintered glass crucible. Next, the purified product was dissolved in water and balanced using a diluted solution of hydrochloric acid, with equal volumes of each. Afterward, the balanced product of the reaction was formed by introducing ethyl alcohol, and two rinses were performed with a methanol-water mixture, with a ratio of 80% methanol to 20% water. This was followed by an additional wash using pure methanol. To prepare the final product for analysis, the precipitated material was primarily dried up at RT followed by drying in vacuum oven at 40°C for duration of 4 hours. This drying process ensured the removal of any remaining solvent or moisture from the product.[13]

Characterization of CMTG

ATR-FTIR of CMTG

The CMTG was placed on the ATR crystal, and the sample was scanned between 600 to 4000 cm^{-1}.

Thermal analysis of CMTG

TGA and DSC of CMTG were conducted utilizing a thermogravimetric analyzer. The samples were subjected to heating between 30 to 500°C.

^{13}C NMR

The CMTG compound was analyzed using solid-state ^{13}C cross-polarization-magic angle spinning NMR. Experimental parameters included a contact time of 3.5 milliseconds, a relaxation delay of 5 seconds.

X-ray diffraction study

The X-ray diffraction study (XRD) of CMTG was attained by utilizing an X-ray diffractometer (PW1729, Philips, The Netherlands) equipped with a copper target. The scanning speed was set at 2°C per minute, and the scanning angle ranged from 0 to 90 degrees (2θ).

Preparation of SD using CMTG as a carrier

VRZ loaded SD using CMTG was prepared by using kneading method at different drug: polymer ratio.[14] First, the required amount of VRZ was melted in an applicable quantity of methanol. Then, the necessary amount of CMTG (another substance) was added to this solution while continuously stirring it in a mortar for duration of 30 minutes. Afterward, the solvent was permissible towards evaporating, resulting in a solidified mass forming. This mass was then subjected to drying, grinding, and passing through a sieve of a size of no. 80 mesh. The solid dispersions prepared in this manner were then characterized. Furthermore, a similar process was followed to manufacture solid dispersions using TG (presumably another substance), and these were compared with the solid dispersions of CMTG (Table 1).

Characterization of SD

Percentage yield

The yield was calculated using below formula.[14]

% Yield = SD Wt/Wt of drug and polymer X 100 ------- (1)

Drug content

SD eq to 10 mg of VRZ was dissolved in a 100 mL methanol (25 mL). The resulting solution was then stirred in a centrifuge for duration of 60 minutes to ensure thorough mixing and dissolution. Afterward, the solution was filtered to remove any particulate matter or impurities. The filtered solution was analyzed at 238 nm to measure the drug content. Methanol was used as a blank in the spectrophotometer, meaning its absorbance was also measured and accounted for in the analysis.

Table 1: Composition of various batches of SD containing CMTG and TG mixture

Batch Code	*Composition*	*Ratio*
SD1	VRZ: TG	1:1
SD2	VRZ: TG	1:2
SD3	VRZ: TG	1:3
SD4	VRZ: CMTG	1:1
SD5	VRZ: CMTG	1:2
SD6	VRZ: CMTG	1:3

Saturation solubility determination

The saturation solubility of the SD and pure VRZ was determined using the shake-flask method. In separate glass-stoppered flasks, plain VRZ and SD containing an excess quantity of VRZ containing distilled water were added. The flasks were subsequently positioned on a magnetic stirrer adjusted to 37°C with stirring at 100 rpm. This stirring process was continued until equilibrium was reached, which took approximately 24 hours. After achieving equilibrium, small portions of the samples (aliquots) were filtered through Whattman No. 41 filter paper to remove any un-dissolved particles. The resulting filtrates were appropriately diluted with distilled water, and samples were analysed at 238 nm.[15]

In-vitro dissolution studies

This study was performed on both plain VRZ and solid dispersion samples (SSDs) utilizing the USP dissolution test apparatus II. To commence the dissolution process, samples containing an equivalent of 20 mg of VRZ were introduced into 900 mL of pH 6.8 phosphate buffer at 37 ± 0.5°C, at 50 rpm. About 5 mL aliquots were withdrawn at each time point and filtered. Sink was maintained by addition of equal volume of buffer. The filtered samples were subjected to spectrophotometric analysis at a wavelength of 238 nm.

Infrared spectroscopy

Infrared spectra of pure voriconazole, and final optimised solid dispersion (SD5) were verified through with FTIR. Small samples were taken and directly put on IR platform and scanning was done from 400 to 4000 cm^{-1}.

Differential scanning calorimetry

Differential scanning calorimetry (DSC) investigation was performed for pure VRZ and solid dispersion formulation (SD5). The samples kept in aluminium pans were sealed. The samples underwent heating at a rate of 10°C per minute, beginning from 25°C and incrementally rising to 500°C. A nitrogen gas was used throughout this heating procedure to prevent any unintended reactions or contamination.

Powder XRD

Powder XRD (P-XRD) examination was conducted to assess the presence of crystallinity at two stages: after the formulation was prepared and after the strength studies were carried out. For the XRD analysis, powdered samples of pure VRZ and the solid dispersion formulation (referred to as SD5) were placed in an aluminum test holder. The test holder had a surface area of 2.5 cm^2 and a specified depth in millimeters.

In-vivo pharmacokinetic study

- *Animal maintenance and handlings*

Healthy, adult male Wister rats (150–200 gm) were used in this study. Animal study was performed as per guidelines

and regulations established by ethical committee. Prior approval was obtained from the committee to ensure ethical compliance in the study (YSPM/YTC/PHARMA-IAEC/201-22/14)

- *Animal grouping and dosing*

Two groups of rats, each consisting of 6 animals, were randomly selected for a study. The rats were subjected to a 12-hour fasting period prior to the experiment. In group I, the rats were given a suspension of pure VRZ (50 mg/kg) prepared with 0.5% methocel. In group II, the rats were administered solid dispersions containing an equivalent dose of voriconazole (50 mg/kg), diluted in 0.5% methocel, through the oral route. At specific time intervals (0, 0.50, 1, 1.50, 2, 2.50, 3, 4, 5, 6, 8, 12, 16, 20, and 24 hours after dosing), 500 µL blood was withdrawn from the retro-orbital plexuses of the rats. These samples were then transferred to Eppendorf tubes comprising heparin towards preventing blood clotting. The plasma separation was done by centrifugation at 5000 rpm for 5 to 10 minutes, then frozen at -20°C pending investigation.

- *Determination of VRZ in rat plasma*

The C18 column with a mobile phase of acetonitrile-water-acetic acid (55:45:0.25, v/v/v) was adjusted to a pH of 4.0. The samples were analysed using UV detector at 256 nm and voriconazole concentration was estimated. The pharmacokinetic area under curve (AUC), Cmax, T_{max}, and $t_{1/2}$ were determined.

- *Formulation of VRZ tablets containing TMCG SD*

Tablets were formulated using direct compression method using excipients listed in Table 2. All excipients were passed through #40 sieve and mixed together properly. Finally, magnesium stearate and talc were passed through #60 sieve, added to previous blend, and lubricated for 5 min. This ready blend was compressed using KBR press.

Characterisation of Blend

Bulk density

The Bulk density was calculated using formula mentioned.

$$BD = \frac{\text{mass of sample in g}}{\text{volume occupied by sample in ml}}$$

Tapped density

The Tapped density was calculated using formula mentioned below

$$TD = \frac{\text{Mass of sample in gm}}{\text{tapped volume occupied by sample in ml}}$$

Compressibility index

Following formula was used to calculate the Compressibility index.

$$CI = \frac{TD - BD}{TD} X\ 100$$

Angle of repose

Following formula was used to calculate the angle f repose.

$$\tan\theta = \frac{h}{r}$$

Hausner's ratio

Following formula was used to calculate the Hausner's ratio.

$$HR = \frac{TD}{BD}$$

Characterisation of Tablets

Tablet thickness

Thickness measurements were conducted on ten tablets randomly chosen from each batch formulation using a screw gauge.

Weight variation

This was determined by calculating average weight of the 20 tablets.

Hardness

The tablets' hardness was assessed using a Monsanto hardness tester.

Friability

Friability testing was performed utilizing Roche's friabilator as per procedure mentioned in official books or literature.

Content uniformity

About 10 tablets were crushed to make powder. Powder eq to 20 mg of VRZ was dissolved in methanol under

Table 2: Formula arrangement of VRZ tablets using SD

Ingredients (mg/tablet)	*F1*	*F2*	*F3*	*F4*	*F5*	*F6*	*F7*	*F8*
SD of VRZ eq. to 50 mg	160	160	160	160	160	160	160	160
Microcrystalline cellulose	60	56.5	53	49.5	46	42.5	39	35.5
Anhydrous lactose	50	50	50	50	50	50	50	50
Fujicalin	67.75	64.25	60.75	57.25	53.75	50.25	46.75	43.25
Croscarmellose sodium	7	14	21	28	35	42	49	56
Magnesium stearate	1.75	1.75	1.75	1.75	1.75	1.75	1.75	1.75
Talc	3.5	3.5	3.5	3.5	3.5	3.5	3.5	3.5
Tablet weight	350	350	350	350	350	350	350	350

continuous shaking. The solution was filtered and analysed at 238 nm to estimate the drug content.

Disintegration time

Disintegration testing was performed on 6 tablets using an apparatus detailed in the United States Pharmacopeia (USP), specifically the Electro lab Disintegration apparatus containing distilled water at a temperature of 37°C ± 2°C.

In-vitro dissolution study

A USP type II apparatus containing 900 mL of pH 6.8 phosphate buffer was used for the dissolution process. The buffer was stirred at 50 rpm while maintaining a temperature of 37.0 ± 0.5°C. About 10 mL samples were taken out at prearranged intervals, and the same amount of new buffer was added. The samples were examined at 238 nm.

RESULTS

Synthesis of CMTG

CMTG offers enhanced water solubility, improved rheological properties, film-forming capabilities, customizable modifications, and increased stability, making it a preferred choice over pure tamarind gum in various industrial applications.[9] TG-alkoxide formation was achieved by adding TG to a methanolic solution containing sodium hydroxide. When this solution was heated in the presence of monochloroacetic acid, a nucleophilic substitution (SN2) reaction occurred between TG-alkoxide and monochloroacetic acid, resulting in the carboxymethylation of TG. The successful carboxymethylation of TG was confirmed using infrared spectroscopy. For the carboxymethylation process, a batch size of 50 grams was used. The percentage yield of carboxymethyl TG was determined to be 50.6 ± 4.17%. The degree of substitution, which indicates the extent of carboxymethylation, was calculated using the titrimetric method and found to be in the range of 0.16 to 0.2. This range represents the average number of carboxymethyl groups attached to each TG molecule.

FTIR Analysis of CMTG

The FTIR spectrum of CMTG presented prominent, broad peaks in the range of 3500 to 3000 cm^{-1}, indicating the stretching vibrations of hydroxyl (-OH) groups present in the polysaccharide. Intermediate intensity peaks at 2856 and 2927 cm^{-1} suggested the presence of asymmetric stretching vibrations of carbon-hydrogen (C-H) bonds. The appearance of a peak at 1745.56 cm^{-1} specified the existence of a carbonyl (C=O) group, specifically from the ester group. Peaks observed at 1639 cm^{-1} and 1402 cm^{-1} provided evidence of carboxyl (-COOH) groups in CMTG. Furthermore, a peak at 1010 cm^{-1} points out the stretching vibrations of the glycosidic link (C-O-C) within CMTG. The carboxymethylation of tamarind gum was confirmed by the presence of distinguishing peaks at 1745.58 (C=O) and 1402 cm^{-1} (-COO-), corresponding to the carboxymethyl group. Different IR peaks of the CMTG are presented in (Fig. 1).

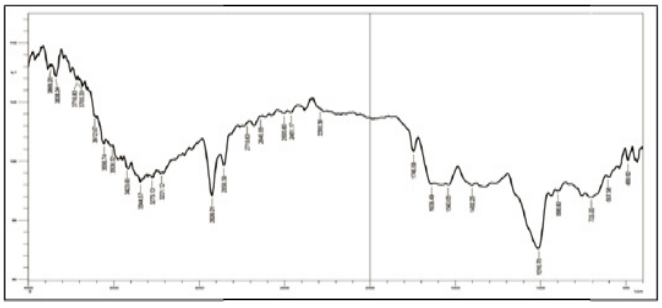

Fig. 1: FTIR spectra of CMTG with different peak

Thermal Analysis of CMTG

The thermal decomposition curve of CMTG displays two primary phases of weight loss (Fig. 2). The chief phase initiates at 35°C and concludes at 100°C, and showed the 3.91% of weight loss. This initial stage is likely associated with the elimination of free as well as bound molecules of water embedded in polymer structure. The second phase accounting for a significant weight loss of 54.42%. This stage marks the initial degradation of the polymer backbone. A significant weight loss of up to 90% occurs at 485°C.

Solid State ^{13}C-NMR of CMTG

The spectrum of CMTG exhibits three discernible peaks. A peak positioned 105.2 ppm is attributed to the molecule's anomeric carbon atom (C1), while another peak at 74.28 ppm corresponds to carbon atoms proximate to hydroxyl (-OH) groups. Specifically, this peak represents the carbon atoms within the six-membered ring, excluding

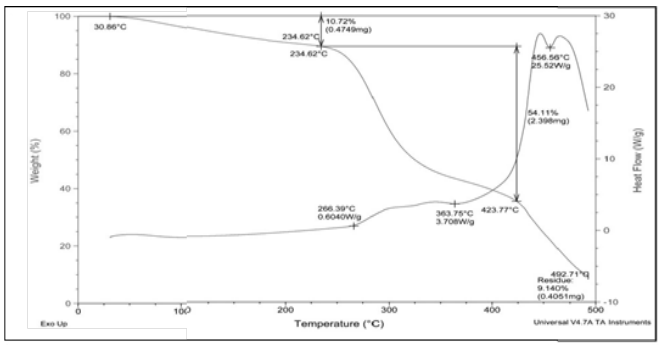

Fig. 2: DSC-TGA of CMTG

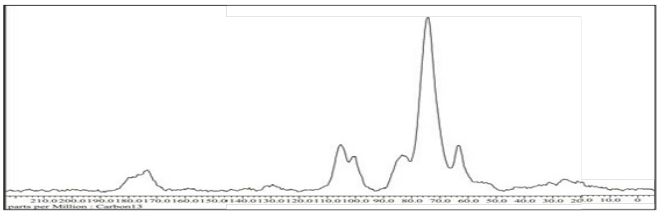

Fig. 3: Solid state ^{13}C-NMR of CMTG

the C1 carbon atom. Additionally, a peak at 63.59 ppm is observed, which resembles in the direction of the C6 carbon atom of the CH_{20}- group in the molecule. Furthermore, a signal is observed at 173.32 ppm, indicating the presence of the carbonyl carbon in CMTG. Interestingly, when examining the solid-state ^{13}C NMR spectrum of the hydrogel film, all the resonance peaks detected in CMTG are also present in (Fig. 3). This suggests that the hydrogel film contains the same chemical groups and structural elements as CMTG, as evidenced by the resonance peaks in the NMR spectrum.

XRD

The XRD (Fig. 4), study indicates a predominantly amorphous nature with no distinct peaks in CMTG. This lack of sharp peaks suggests the absence of well-defined crystalline regions and implies that the polymer chains are randomly arranged, resulting in a disordered structure. A weak peak denotes a low degree of crystallinity and the presence of tiny crystalline areas within the amorphous matrix.

Development of VRZ-loaded SD

CMTG has been explored as a carrier for SD formulations by kneading method. This technique is employed to prepare solid dispersions by mechanically mixing the drug and carrier in the existence of an appropriate solvent.[16] CMTG, as a hydrophilic polymer, can enhance the aqueous solubility of the drug molecules with very limited solubility.[17]

%Yield and Drug Content

A higher SD yield (93.0–97.51%) was observed in all formulation batches with TG and CMTG. The details of the yield are presented in (Table 3). High yield indicated the minimum defeat of the excipients and drug throughout the production method. The kneading process involves prolonged and intensive mechanical mixing of the drug and polymer.[18] This enhanced interaction facilitates better dispersion of the drug within the polymer matrix, leading to improved drug dissolution. The increased drug-polymer interaction, reduced particle size, and homogeneous distribution contribute significantly to the higher yield observed in solid dispersions prepared using this method. Moreover, these factors also enhance drug solubility, further enhancing the efficacy of the formulation. The drug content of the SD was also found to be higher (94.77–97.88%) in all the formulated batches. The kneading process helps in achieving a more uniform distribution of the drug within the polymer matrix.

Table 3: Comparative yield of the SD formulated using kneading method

Batch Code	*Composition*	*Ratio*	*%Yield*	*%Drug content*
SD1	VRZ: TG	1:1	93.00	94.77
SD2	VRZ: TG	1:2	94.89	94.81
SD3	VRZ: TG	1:3	96.45	95.24
SD4	VRZ: CMTG	1:1	97.51	96.51
SD5	VRZ: CMTG	1:2	94.57	97.24
SD6	VRZ: CMTG	1:3	95.42	97.88

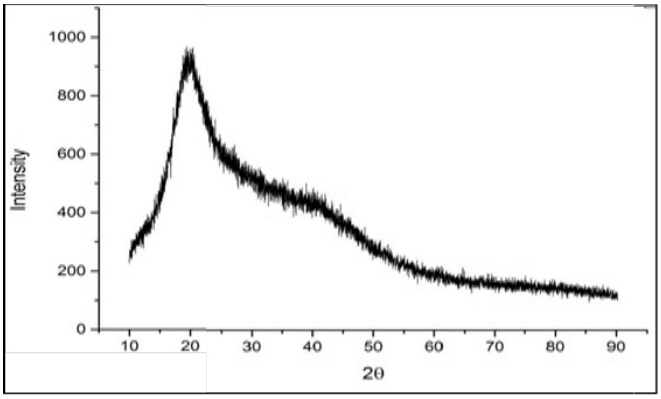

Fig. 4: XRD of CMTG

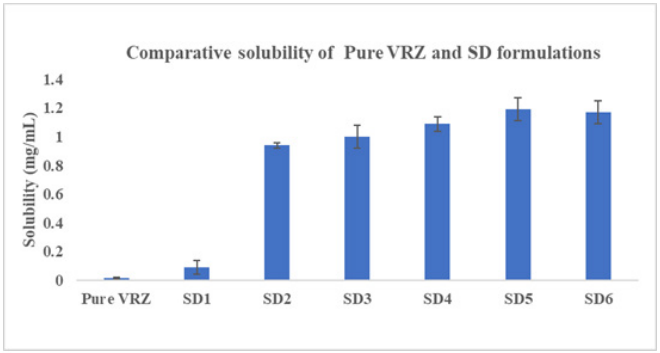

Fig. 5: Comparative saturation solubility of VRZ and SD in distleed water

Saturation Solubility Determination

Tremendous improvement in solubility was found with SD formulations in comparison to pure VRZ. The comparative solubility data is presented in (Table 4 and Fig. 5). SD of VRZ prepared with TG exhibited a solubility enhancement ranging from 5.62 to 62.5-fold in water. Conversely, SD prepared with CMTG demonstrated a significantly higher solubility enhancement, ranging from

Table 4: Saturation solubility data of the VRZ and SD formulations in distilled water

Batch Code	*Formulation/ Components*	*Ratio*	*Solubility (mg/mL)*	*Fold enhancement*
---	Pure VRZ	---	0.016	.....
SD1	VRZ: TG	1:1	0.09	5.62
SD2	VRZ: TG	1:2	0.94	58.75
SD3	VRZ: TG	1:3	1.00	62.5
SD4	VRZ: CMTG	1:1	1.09	68.12
SD5	VRZ: CMTG	1:2	1.19	74.37
SD6	VRZ: CMTG	1:3	1.17	73.12

68.12 to 74.37-fold. These results unequivocally indicate that CMTG possesses superior potential for enhancing the solubility of VRZ compared to TG. CMTG may exhibit stronger interactions with VRZ compared to TG due to differences in their chemical structure or functional groups. The improved interaction facilitates enhanced drug dispersion and increased solubility within the solid dispersion. Additionally, CMTG might exhibit superior wetting and dispersion characteristics when compared to TG.[4] This may result in improved VRZ dispersibility in the solid dispersion leading to enhancement of the solubility.

In-vitro Dissolution Studies

Dissolution investigations were accompanied towards comparing the dissolution profiles of plain VRZ and SSDs. The results of the dissolution profiles for pure VRZ and the SD formulations are presented (Fig. 6). In the pure drug sample, 39% of the VRZ was dissolved, but after 120 minutes, the SD5 formulation demonstrated full release from the solid dispersion. When compared to the SDs of TG, the SDs produced with CMTG exhibited a quicker release profile. It was found that the best ratio for forming the SD of VRZ was 1:1 for the SD5 formulation. When compared to TG, CMTG in solid dispersions with VRZ shows better drug-polymer interaction, dispersibility, and wetting.[4] It enhances drug release by increasing surface area, improving drug dispersion, and solubilization. By maintaining VRZ in a supersaturated condition, CMTG increases the effective drug concentration and facilitates a quicker rate of dissolution. Increased solubility and dissolution rates are made possible by enhanced miscibility, which guarantees uniform medication distribution. Overall, CMTG solid dispersions result in enhanced VRZ dissolution kinetics. At higher concentration of CMTG, i.e., 1:3 ratio establishes towards retarding the release of drug form SDs. Higher concentrations of CMTG in voriconazole solid dispersions result in a thick polymer matrix that acts as a diffusion barrier to impede drug release. Drug release is hindered by stronger polymer-drug interactions, which restrict diffusion and dissolution. Additionally, at higher concentrations, CMTG may undergo swelling or gel formation, creating a physical barrier that delays drug diffusion.[19] These factors contribute to a slower and sustained drug release profile in CMTG solid dispersions at higher concentrations.

FTIR of VRZ SD

The FTIR of pure VRZ shows aromatic C-H stretching vibrations in the province of 3000 to 3100 cm^{-1}, indicating the presence of aromatic rings in the molecule (Fig. 7). Aliphatic C-H stretching vibrations were observed between 2800 to 3000 cm^{-1}. The carbonyl (C=O) stretching vibration appears as a sharp peak in the 1650 to 1750 cm^{-1} area, representing the existence of carbonyl groups in the molecule. The triazole ring vibrations, characteristic of VRZ's structure, can be identified by absorption bands

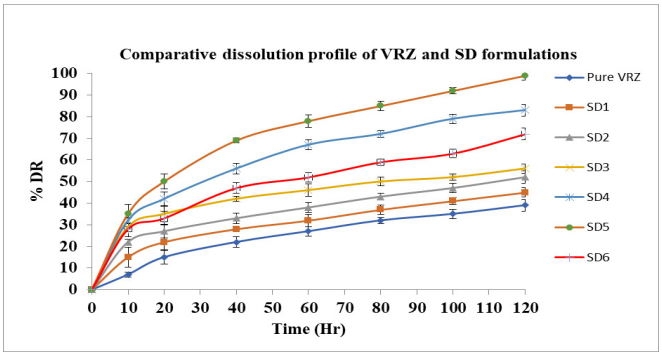

Fig. 6: Comparative dissolution profile of the pure VRZ and SD formulations in pH 6.8 phosphate buffer

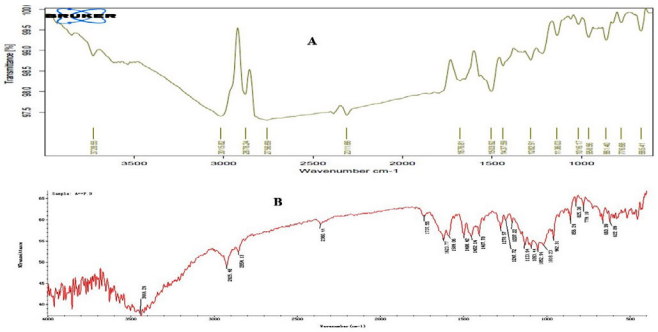

Fig. 7: FTIR spectra of (A) Pure VRZ and (B) SD of VRZ

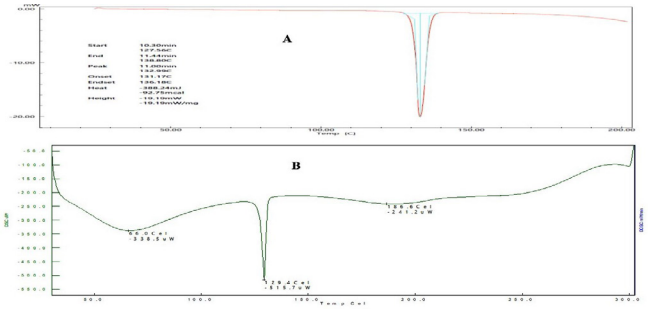

Fig. 8: DSC thermogram of (A) Pure VRZ and (B) Solid dispersion SD5

in the 1500 to 1600 cm^{-1} region. These vibrations are specific to the triazole moiety. The spectrum also shows absorption bands within the 1000 to 1400 cm^{-1} range, indicating vibrations associated with nitrogen-containing heterocycles. Voriconazole contains multiple nitrogen-containing heterocycles, and these vibrations provide further confirmation of the compound's structure. The hydroxyl (OH) groups present in the molecule, their stretching vibrations can be observed in the region of 3200 to 3600 cm^{-1}. Similar peaks were also detected in the SD FITR spectra (Fig. 7).

DSC Study of VRZ SD

The DSC thermograms of the SD5 formulation and pure VRZ are presented in Figs 8A and 8B, respectively. Pure VRZ showed a distinct endothermic peak at 132.99°C, indicating its crystalline nature. The melting point of

pure VRZ, which is normally between 129 and 134°C, is represented by this peak. However, the solid dispersion formulation's (SD5) showed peak at 129.40°C. When compared to pure VRZ, the strength of the endothermic peak for VRZ in the SD formulation is lower. The decrease in peak intensity indicates that VRZ in the solid dispersion formulation is becoming more amorphous. Overall, the DSC analysis provides insights into the thermal behavior and crystallinity of the pure VRZ and SD5 formulation, indicating the presence of an amorphous component in the solid dispersion formulation.

XRD Analysis of VRZ SD

VRZ's prominent and clear peaks may be seen in the XRD spectrum displayed in Fig. 9A at diffraction angles of 27.50, 29.90, 31.7, 45.2, 57.5, 66.4, and 75.2 degrees. This suggests that pure VRZ is crystalline. The strength of VRZ crystalline peaks is much lower in the SD5 formulation seen in (Fig. 9B). This suggests that VRZ occurs in an amorphous state in the final formulation. These results offer convincing proof that VRZ was effectively converted to amorphous from in SD formulation.

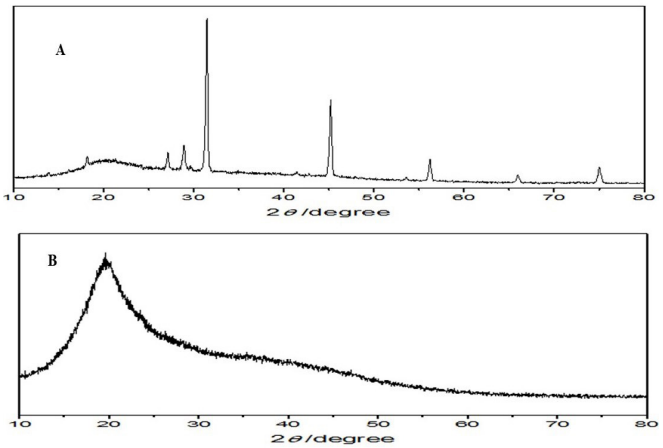

Fig. 9: X ray diffraction pattern of (A): Pure VRZ drug and (B): SD5 formulation

SEM Analysis of VRZ SD

The morphology and particle properties of the VRZ loaded CMTG SD were examined using SEM. The distribution and physical makeup of the medication within the CMTG matrix were better understood thanks to the SEM pictures. The SEM picture showed that the solid dispersion of CMTG loaded with VRZ had a different shape from the pure components. The VRZ dispersed particles were visible as tiny, asymmetrical particles incorporated into the CMTG matrix (Fig. 10). The drug particles were encircled by a continuous, amorphous structure that was the CMTG matrix. The solid dispersion, in which the medication was distributed inside the polymeric carrier, had been successfully developed, according to the SEM analysis. The presence of VRZ particles dispersed in the CMTG matrix indicated good compatibility and interface amongst the drug and the polymer. Overall, the SEM study showed that the CMTG carrier successfully distributed VRZ and created a solid dispersion. The images provided valuable details regarding the morphology, particle size, and distribution of the drug within the CMTG matrix, supporting the understanding of the solid dispersion's structure and potential impact on the dissolution behavior of VRZ.

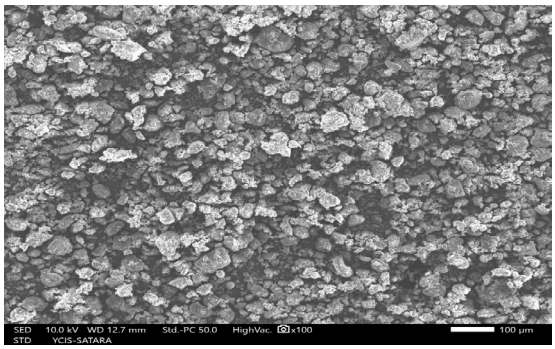

Fig. 10: SEM of VRZ loaded CMTG solid dispersion

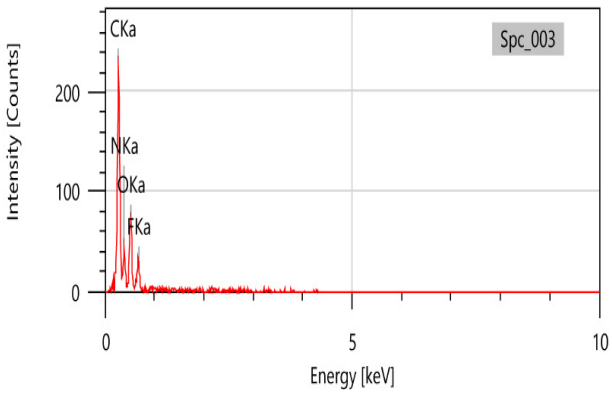

Fig. 11: EDS analysis of SD5 formulation with intensity count and energy

Energy-Dispersive X-ray Analysis

Energy-dispersive X-ray spectroscopy is a very helpful analytical technique for determining a material's elemental makeup. Understanding the substance's characteristics and chemical structure requires understanding these specifics. The specific elements present in the VRZ loaded CMTG solid dispersion using energy-dispersive X-ray spectroscopy are carbon (C), a fundamental element found in organic compounds, including voriconazole and the CMTG polymer. Hydrogen (H) is another essential element found in organic compounds, including VRZ and the CMTG polymer. Oxygen (O) is commonly present in organic molecules as well as in the CMTG polymer, which may contain hydroxyl (-OH) groups. Nitrogen (N) was also present in VRZ, which contains a triazole ring that includes nitrogen atoms. Florine (F) is constituent of VRZ, as it contains a chlorine atom in its chemical structure (Fig. 11).

In-vivo Pharmacokinetic Study

Fig. 12, illustrates the comparison between VRZ SD formulation and VRZ pure suspension in wistar rats. Rats that received the solid dispersion formulation had plasma concentrations of voriconazole that were noticeably greater than those of rats administered with the pure drug suspension over the course of the designated intervals of time. After giving the two formulations of VRZ to wistar rats orally, (Table 5) shows the plasma pharmacokinetic properties of the drug.

The results presented in the above table demonstrate that the VRZ SD formulation exhibited higher values of AUC and C_{max} associated to the pure drug formulation. Specifically, the AUC for the solid dispersion formulation was measured to be approximately 10.26 ± 0.08 µg.hr/mL, while the C_{max} was determined to be 0.964 ± 0.01 µg/mL. These values were meaningfully higher ($p < 0.05$) than those observed for the pure drug suspension formulation, which had a C_{max} of 0.456 ± 0.05 µg/mL. The solid dispersion formulation and pure drug suspension had different values for T_{max}, with the solid dispersion formulation exhibiting a T_{max} of 2.00 ± 0.05 hours, while the pure drug suspension had a Tmax of 3.00 ± 0.07 hours. The $AUC_{0-\infty}$ of SD was higher at 10.26 ± 0.08 µg hmL^{-1}, equated to the pure drug suspension formulation which had an $AUC_{0-\infty}$ of 4.77 ± 0.06 µg hmL^{-1}. Furthermore, differences that are statistically significant ($p < 0.05$) were observed in the AUC_{0-t} between the SD formulation and the pure drug suspension formulation. Compared to the pure drug solution formulation, the solid dispersion formulation of VRZ has a more effective systemic absorption, as seen by the greater drug concentration in the blood. This suggests that the solid dispersion formulation enhances the bioavailability of VRZ by improving its absorption into the systemic circulation.[20]

Table 5: Pharmacokinetic characteristics of voriconazole solid solid dispersions formulation and pure drug

Pharmacokinetic characteristics	*Voriconazole pure drug*	*Voriconazole- solid dispersions*
C_{max} (µg/mL)	0.456 ± 0.05	0.964 ± 0.01
AUC_{0-t} (µg.hr/mL)	3.01 ± 0.05	9.41 ± 0.09
AUC_{0-inf} (µg.hr/mL)	4.77 ± 0.06	10.26 ± 0.08
T_{max} (hr)	3.00 ± 0.07	2.00 ± 0.05
$t_{1/2}$ (hr)	6.43 ± 0.08	4.26 ± 0.04

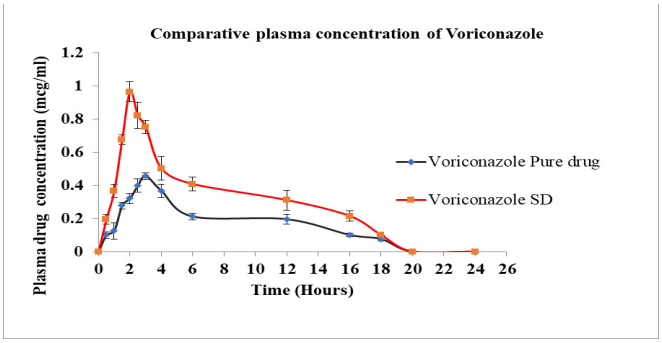

Fig. 12: Comparative plasma concentration of voriconazole form SD and pure drug

Evaluation of Lubricated Blend

The lubricated blend's flow characteristics are shown in (Table 6). The granules' angle of repose varied from 27.01 ± 0.34 to 39.42 ± 0.42, their BD ranged from 0.46 ± 0.003 to 0.70 ± 0.003 gm/cm^3, and their TD ranged from 0.54 ± 0.001 to 0.84 ± 0.004. The HR varied between 1.16 ± 0.002 and 1.32+0.001, while the CI was determined to be between 14.46 ± 0.1 and 24.61 ± 0.21. Based on all the parameters examined, batch F5 demonstrated excellent flow characteristics in this study. Additionally, the lubricated blend of batches F6 showed superior flow characteristics as seen by the higher BD values, which directly impacted the lubricated blend's HR and Carr's index CI. HR values between 1.00 and 1.11 and CI values ranging from 0 to 10 are indicative of exceptional powder flow properties.[21]

Evaluation of Tablets of VRZ

Round punch with diameter of 10 mm was used to compress the tablets. The diameter of the compressed tablets was found 10.04 ± 0.03 to 10.08 ± 0.04 mm (Table 7). The tablet diameter was found to be acceptable considering the dimensions of the of the punch. Very less weight variation

Table 6: Flow properties of the lubricated blend containing SD of VRZ

Batch	*BD (gm/mL)*	*TD (gm/mL)*	*CI (%)*	*HR*	*Angle of repose*
F1	0.48 ± 0.003	0.56 ± 0.003	24.61 ± 0.21	1.16 ± 0.004	27.17 ± 0.16
F2	0.48 ± 0.002	0.63 ± 0.002	24.61 ± 0.2	1.32+0.001	35.61 ± 0.21
F3	0.46 ± 0.04	0.54 ± 0.001	17.55+0.2	1.21+0.005	39.42 ± 0.42
F4	0.46 ± 0.003	0.56 ± 0.001	16.39+0.21	1.19+0.001	36.62 ± 0.12
F5	0.70 ± 0.003	0.84 ± 0.004	8.32 ± 0.1	1.10 ± 0.002	27.01 ± 0.34
F6	0.67 ± 0.002	0.84 ± 0.001	20.52+0.12	1.25+0.001	28.91+0.31
F7	0.47 ± 0.01	0.58+0.002	18.43 ± 0.12	1.22 ± 0.002	31.33 ± 0.16
F8	0.48 ± 0.004	0.63 ± 0.004	22.17 ± 0.15	1.20 ± 0.001	28.27 ± 0.12

Table 7: Comparative physicochemical properties of the compressed tablets

Batch	Thickness (mm)	Diameter (mm)	Hardness (kg/cm^2)	Friability (%)	Weight variation	Content uniformity	DT	Water absorption (%)
F1	2.98 ± 0.057	10.05 ± 0.03	4.16 ± 0.15	0.19	350.80 ± 0.96	97.14 ± 1.20	80.32 ± 1.62	72.24 ± 0.55
F2	3.10 ± 0.1	10.03 ± 0.02	4.25 ± 0.15	0.20	349.02 ± 1.05	98.12 ± 1.72	78.15 ± 1.0	73.56 ± 0.47
F3	2.89 ± 0.05	10.08 ± 0.04	4.30 ± 0.15	0.15	350.92 ± 1.06	98.26 ± 1.42	71.01 ± 1.2	90.34 ± 0.01
F4	3.12 ± 0.07	10.06 ± 0.05	4.15 ± 0.05	0.26	349.60 ± 1.09	97.11 ± 1.30	65.35 ± 2.0	78.26 ± 0.03
F5	2.97 ± 0.05	10.07 ± 0.04	5.15 ± 0.35	0.29	348.50 ± 0.85	100.05 ± 0.99	54.27 ± 1.0	93.42 ± 0.68
F6	2.89 ± 0.05	10.04 ± 0.03	5.00 ± 0.11	0.16	350.25 ± 1.07	98.67 ± 1.26	66.32 ± 1.4	88.39 ± 0.38
F7	2.98 ± 0.05	10.05 ± 0.02	4.95 ± 0.28	0.23	351.10 ± 1.02	99.98 ± 1.12	72.25 ± 1.0	86.48 ± 0.66
F8	3.01 ± 0.057	10.05 ± 0.04	4.90 ± 0.76	0.30	351.24 ± 0.99	99.78 ± 1.27	80.11 ± 1.5	76.78 ± 0.10

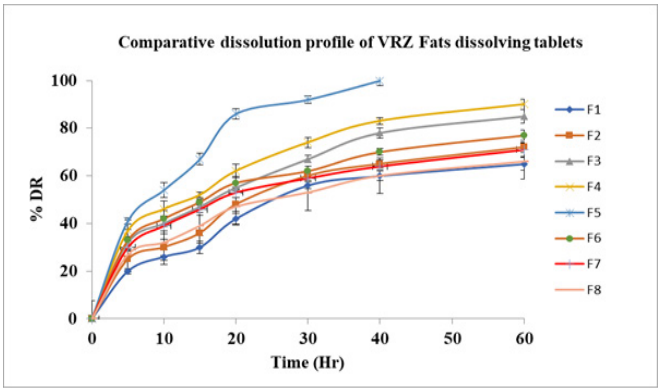

Fig. 13: Comparative dissolution profile of VRZ from fast dissolving tablets

Table 8: Comparative dissolution profile of fast dissolving tablets containing VRZ SD

Time (min)	*Formulations*							
	F1	*F2*	*F3*	*F4*	*F5*	*F6*	*F7*	*F8*
0	0	0	0	0	0	0	0	0
5	20	25	32	37	41	33	30	27
10	26	30	40	46	54	42	39	32
15	30	36	47	52	67	49	46	39
20	42	48	55	62	86	57	53	47
30	56	60	67	74	92	62	59	53
40	60	65	78	83	100	70	64	60
60	65	72	85	90	.....	77	71	66

ranging was observed. The excellent content uniformity was observed ranging from 100.05 ± 0.99 to 97.11 ± 1.30.[22] Hardness was fond between 4.15 ± 0.05 to 5.15 ± 0.35 kg/cm^2. Using a Roche friabilator, the tablets' friability was assessed, and it was found to be within an acceptable range of 0.15 to 0.30% (less than 1%). It was discovered that the tablets' thickness ranged from 2.89 ± 0.05 to 3.12 ± 0.07 mm. All formulations had an *in-vitro* disintegration time that ranged from 54.27 ± 1.0 to 80.32 ± 1.62 seconds. The effect of croscarmellose sodium (CCS) was found to be concentration dependent up to 10%. Beyond this concentration, the DT was found to be increased due to gelling property of CCS at higher concentrations. Water absorption was found to be 72.24 to 93.42% depending on the concentration of superdisintegrant. It may be due to the hydrophilic nature of carriers used.

Dissolution of VRZ Compressed Tablets

The comparative dissolution profile is presented in (Table 8 and Fig. 13). All formulation batches were shown to have better dissolving characteristics than the drug release reported in solid dispersions. This improvement in dissolution rate was attributed to the presence of the superdisintegrant CCS. The effect of CCS on dissolution was observed to be concentration dependent, up to a concentration of 10%, similar to disintegration time (DT).[23] However, beyond this concentration, the dissolution of VRZ was observed to decline (Fig. 13). F5 exhibited excellent fast-dissolving potential among the formulations, achieving complete drug release within 40 minutes. Formulations with CCS concentrations above 10% (F6 to F8) demonstrated 77 to 66% drug release within 60 minutes.

Discussion

This study aimed to enhance the solubility, dissolution, and bioavailability of VRZ, a BCS II class drug, by synthesizing CMTG and developing SD using the kneading method. Characterization techniques including FTIR, DSC-TGA, and ^{13}C-NMR confirmed the successful synthesis of CMTG and the formation of SD. XRD analysis revealed the amorphous structure of CMTG, contributing to its solubilizing properties. Compared to traditional methods, SD formulated with CMTG exhibited a remarkable increase in solubility enhancement. In vivo studies in rat models further validated the enhanced bioavailability of VRZ with SD administration, highlighting the potential of this approach in optimizing drug delivery systems.

In this work, CMTG was created from TG and used to carry VRZ in a solid dispersion. The solid dispersion formulated with CMTG exhibited improved dissolution profiles

compared to solid dispersions formulated with TG alone. The optimised SD showed enhanced pharmacokinetic parameters in comparison to pure VRZ. Multiple causes were identified as the cause of this improvement. First, better dissolution rates were attained by increasing the drug's solubility through the amorphous form of VRZ, which was obtained due to the matrix formation. The finely dispersed VRZ particles within the CMTG matrix increased the surface area, facilitating more efficient drug dissolution upon contact with the dissolution medium.

CMTG acted as a carrier and provided a protective environment for VRZ, preventing agglomeration and recrystallization, which can hinder dissolution.[24] Additionally, CMTG potentially formed hydrogen bonds with the drug molecules, further enhancing their solubility and dissolution. Furthermore, when the optimized CMTG solid dispersion was incorporated into fast-dissolving tablets, the addition of CCS as a superdisintegrant further improved the dissolution rate. CCS facilitated quick disintegration of the tablet following touch with saliva, rapidly releasing the dispersed VRZ. The combination of CMTG and CCS synergistically improved the dissolution rates of VRZ within the tablets, up to a concentration of 10% CCS. Amount of CCS beyond 10% resulted in a decline in the dissolution of VRZ. This decline could be attributed to factors such as increased viscosity, gel formation, tablet hardness, and limited water penetration, which can impede drug release. In summary, the study demonstrated that the synthesis of CMTG and its utilization in SD as carrier improved the drug's solubility, surface area, and dissolution rate. Incorporating the optimized CMTG solid dispersion into fast-dissolving tablets and adding CCS up to 10% concentration further enhanced the dissolution rate. However, concentrations of CCS beyond 10% negatively affected drug release, possibly due to various factors limiting dissolution.

Higher concentrations of CCS in fast-dissolving tablets can have several negative effects on drug release. Firstly, it increases the viscosity of the tablet matrix, creating a physical barrier that hampers the diffusion of drug molecules, leading to slower or restricted drug release.[25] Secondly, CCS can form a gel-like network at higher concentrations when exposed to water or saliva, further impeding drug diffusion and dissolution.[26] Thirdly, increased CCS concentration contributes to greater tablet hardness, which can hinder disintegration and dissolution, resulting in decreased drug release. Lastly, higher CCS concentrations can lead to a more compact and less porous tablet structure, limiting water penetration, which is essential for rapid disintegration and drug dissolution. In summary, higher concentrations of CCS can impede drug release by increasing viscosity, forming a gel network, increasing tablet hardness, and limiting water penetration. Overall, the scientific rationale behind utilizing CMTG in the formulation of VRZ fast-dissolving tablets lies in its ability to enhance solubility, increase surface area, and act as a carrier for the drug. When combined with the superdisintegrant CCS, these formulations exhibit improved dissolution profiles, providing potential benefits for the rapid and effective delivery of VRZ.

Conclusion

The present investigation involved the synthesis of CMTG from TG in SD as carrier for VRZ. SD has significantly improved the solubility and bioavailability of pure drug. This study confirmed the use of CMTG as a potential carrier for VRZ in the form of SD-containing tablets. More studies are required to investigate fully how CMTG and CCS can enhance the therapeutic effectiveness and bioavailability of VRZ and other poorly soluble medications.

Acknowledgment

We are thankful to KES's, Rajarambapu College of Pharmacy, Kasegaon for providing best of facility.

References

1. Peyton LR, Gallagher S, Hashemzadeh M. Triazole antifungals: a review. Drugs Today. 2015; 51(12):705-718.
2. Soe HM, Kerdpol K, Rungrotmongkol T, Pruksakorn P, Autthateinchai R, Wet-Osot S, Loftsson T, Jansook P. Voriconazole Eye Drops: Enhanced Solubility and Stability through Ternary Voriconazole/Sulfobutyl Ether β-Cyclodextrin/Polyvinyl Alcohol Complexes. Int. J. Mol. Sci. 2023; 24(3):2343.
3. Pawar SR, Barhate SD. Solubility enhancement (Solid Dispersions) novel boon to increase bioavailability. J. drug deliv. ther. 2019; 9(2):583-590.
4. Teixeira-Costa BE, Andrade CT. Natural polymers used in edible food packaging—History, function and application trends as a sustainable alternative to synthetic plastic. Polysaccharides. 2022; 3(1):32-58.
5. Idrees H, Zaidi SZ, Sabir A, Khan RU, Zhang X, Hassan SU. A review of biodegradable natural polymer-based nanoparticles for drug delivery applications. Nanomaterials. 2020; 10(10):1970.
6. Malviya R, Sundram S, Fuloria S, Subramaniyan V, Sathasivam KV, Azad AK, Sekar M, Kumar DH, Chakravarthi S, Porwal O, Meenakshi DU. Evaluation and Characterization of Tamarind Gum Polysaccharide: The Biopolymer. Polymers. 2021;13(18):3023.
7. Yamatoya K, Tabuchi A, Suzuki Y, Yamada H. Tamarind seed polysaccharide: unique profile of properties and applications. Biopolymer-Based Formulations. 2020; 445-461.
8. Shukla AK, Bishnoi RS, Kumar M, Fenin V, Jain CP. Applications of tamarind seeds polysaccharide-based copolymers in controlled drug delivery: An overview. Asian J. Pharm. Pharmacol. 2018; 4:23-30.
9. Kumar CS, Bhattacharya S. Tamarind seed: properties, processing and utilization. Crit. Rev. Food Sci. Nutr. 2008; 48(1):1-20.
10. Nayak AK, Pal D. Functionalization of tamarind gum for drug delivery. Funct. biopolym. 2018; 25-56.
11. Warkar SG. Potential applications and various aspects of polyfunctional macromolecule-carboxymethyl tamarind kernel gum. Eur. Polym. J. 2020; 140:110042.
12. Badwaik HR, Kumari L, Maiti S, Sakure K, Nakhate KT, Tiwari V, Giri TK. 2022. A review on challenges and issues with carboxymethylation of natural gums: The widely used excipients for conventional and novel dosage forms. Int. J. Biol. Macromol. 2022;11-15.
13. Goyal P, Kumar V, Sharma P. 2007. Carboxymethylation of tamarind kernel powder. Carbohydr. Polym. 2020; 69(2):251-255.
14. Alwossabi AM, Elamin ES, Ahmed EM, Abdelrahman M. Solubility

enhancement of some poorly soluble drugs by solid dispersion using Ziziphus spina-christi gum polymer. Saudi Pharm J. 2022; 30(6):711-725.
15. Pardeshi SR, More MP, Patil PB, Mujumdar A, Naik JB. Statistical optimization of voriconazole nanoparticles loaded carboxymethyl chitosan-poloxamer based in situ gel for ocular delivery: In vitro, ex vivo, and toxicity assessment. Drug Deliv. Transl. 2022; 12(12):3063-3082.
16. Vasconcelos T, Marques S, das Neves J, Sarmento B. Amorphous solid dispersions: Rational selection of a manufacturing process. Adv. Drug Deliv. Rev. 2016; 100:85-101.
17. Kolimi P, Youssef AA, Narala S, Nyavanandi D, Dudhipala N, Bandari S, Repka MA. Development and characterization of itraconazole non-aqueous creams for the treatment of topical fungal infections. J. Drug Deliv. Sci. Technol. 2022;76:103818.
18. Kulkarni NS, Gite PD, Munde MK, Dhole SN, Khiste RH. A comprehensive review on application of microwave irradiation for preparation of inclusion complexes with cyclodextrins. Res J Pharm Technol. 2021; 14(2):1131-1136.
19. Chowhan A, Giri TK. Polysaccharide as renewable responsive biopolymer for in situ gel in the delivery of drug through ocular route. Int. J. Biol. Macromol. 150:559-572.
20. AboulFotouh K, Zhang Y, Maniruzzaman M, Williams III RO, Cui Z. Amorphous solid dispersion dry powder for pulmonary drug delivery: Advantages and challenges. Int. J. Pharm. 2020; 587:119711.
21. Irigoiti Y, Yamul DK, Navarro AS. Co-crystallized sucrose with propolis extract as a food ingredient: Powder characterization and antioxidant stability. LWT. 2021; 143:111164.
22. Nyavanandi D, Narala S, Mandati P, Alzahrani A, Kolimi P, Almotairy A, Repka MA. Twin Screw Melt Granulation: Alternative Approach for Improving Solubility and Permeability of a Non-steroidal Anti-inflammatory Drug Ibuprofen. AAPS PharmSciTech. 2023;24(1):47.
23. Basu B, Bagadiya A, Makwana S, Vipul V, Batt D, Dharamsi A. Formulation and evaluation of fast dissolving tablets of cinnarizine using superdisintegrant blends and subliming material. J. Adv. Pharm. Technol. Res. 2011; 2(4):266-272.
24. Yadav I, Rathnam VS, Yogalakshmi Y, Chakraborty S, Banerjee I, Anis A, Pal K. Synthesis and characterization of polyvinyl alcohol-carboxymethyl tamarind gum based composite films. Carbohydr. Polym. 2017; 165:159-68.
25. Chen YD, Liang ZY, Cen YY, Zhang H, Han MG, Tian YQ, Zhang J, Li SJ, Yang DS. Development of oral dispersible tablets containing prednisolone nanoparticles for the management of pediatric asthma. Drug Des Devel Ther. 2015; 9:5815.
26. Lavanya DK, Kulkarni PK, Dixit M, Raavi PK, Krishna LN. Sources of cellulose and their applications—A review. Int. J. Drug Dev. Res. 2011; 2(6):19-38.

HOW TO CITE THIS ARTICLE: Velhal AB, Salunkhe VR. Formulation and Development of Voriconazole Tablets Containing Solid Dispersion with Enhanced Solubility, Dissolution and Bioavailability. Int. J. Pharm. Sci. Drug Res. 2024;16(2):220-231. **DOI:** 10.25004/IJPSDR.2024.160212